Biogenic processes in crystalline bedrock fractures indicated by carbon isotope signatures of secondary calcite

Elina Sahlstedt[a], Juha A. Karhu[a], Petteri Pitkänen[b], Martin Whitehouse[c]

[a] Department of Geosciences and Geography, University of Helsinki, P.O. Box 64, 00014 Helsinki, Finland, Emails: elina.sahlstedt@helsinki.fi or juha.karhu@helsinki.fi

[b] Posiva Oy, Olkiluoto, 27160 Eurajoki, Finland, Email: petteri.pitkanen@posiva.fi

[c] Department of Geosciences, Swedish Museum of Natural History, P.O. Box 50 007, SE-10405 Stockholm, Sweden, Email: martin.whitehouse@nrm.se

Corresponding author: Elina Sahlstedt, phone: +358-504480225, fax: +358-9-191-50826

Abstract

Variation in $^{13}C/^{12}C$-isotope ratios of fracture filling calcite was analyzed in situ to investigate carbon sources and cycling in fractured bedrock. The study was conducted by separating sections of fracture fillings, and analyzing the $^{13}C/^{12}C$-ratios with secondary ion mass spectrometry (SIMS). Specifically, the study was aimed at fillings where previously published sulfur isotope data indicated the occurrence of bacterial sulfate reduction. The results showed that the $\delta^{13}C$ values of calcite were highly variable, ranging from -53.8‰ to +31.8‰ (VPDB). The analysis also showed high variations within single fillings of up to 39‰. The analyzed calcite fillings were mostly associated with two calcite groups, of which Group 3 represents possible Paleozoic fluid circulation, based on comparison with similar dated coatings within the Baltic Shield and the succeeding Group 1-2 fillings represent late-stage, low temperature mineralization and are possibly late Paleozoic to Quaternary in age. Both generations were associated with pyrite with $\delta^{34}S$ values indicative of bacterial sulfate reduction. The $\delta^{13}C$ values of calcite, however, were indicative of geochemical environments which were distinct for these generations. The $\delta^{13}C$ values of Group 3 calcite varied from -22.1‰ to +11‰, with a distinct peak at -16‰ to -12‰. Furthermore, there were no observable depth dependent trends in the $\delta^{13}C$ values of Group 3 calcite. The $\delta^{13}C$ values of Group 3 calcite were indicative of organic matter degradation and methanogenesis. In contrast to the Group 3 fillings, the $\delta^{13}C$ values of Group 1-2 calcite were highly variable, ranging from -53.8‰ to +31.8‰ and they showed systematic variation with depth. The near surface environment

of <30 m (bsl) was characterized by $\delta^{13}C$ values indicative of degradation of surface derived organic matter, with $\delta^{13}C$ values ranging from -30.3‰ to -5.5‰. The intermediate depth of 34-54 m showed evidence of localized methanotrophic activity seen as anomalously ^{13}C depleted calcite, having $\delta^{13}C$ values as low as -53.8‰. At depths of ~60-400 m, positive $\delta^{13}C$ values of up to +31.8‰ in late-stage calcite of Group 1-2 indicated methanogenesis. In comparison, high CH_4 concentrations in present day groundwaters are found at depths of >300 m. One sample at a depth of 111 m showed a transition from methanogenetic conditions (calcite bearing methanogenetic signature) to sulfate reducing (precipitation of pyrite on calcite surface), however, the timing of this transition is so far unclear. The results from this study gives indications of the complex nature of sulfur and carbon cycling in fractured crystalline environments and highlights the usefulness of in situ stable isotope analysis.

1. Introduction

Subsurface life and associated geochemical processes usually rely on the circulation of organic and inorganic substrates in groundwater. This is especially true for crystalline bedrock environments, where the bulk of groundwater flow occurs in channels provided by fracture networks. Microbial communities found in these environments are both active and variable (e.g. Bomberg et al., 2015 Hallbeck and Pedersen, 2008; Nyyssönen et al., 2012; Pedersen et al., 2008, 2013). A study by Pedersen et al., (1997) found fossil remains of microbial material in fracture fillings and showed that microbial life in crystalline environments may have ancient roots. Most of dissolved organic matter introduced into the fractured rock via infiltrating waters will be mineralized by aerobic and anaerobic microbial processes, which, in turn, may lead to fracture mineral precipitation (e.g. Drake et al., 2015a, b; Sahlstedt et al., 2013). In fractured rock, early hydrothermal fillings generally dominate fracture mineralizations (Blyth et al., 2000, 2009; Drake and Tullborg, 2009; Sandström and Tullborg, 2009; Sahlstedt et al., 2010). However, late low temperature fillings commonly occur and mineral phases such as calcite can provide an important record of paleofluid circulation in the bedrock (e.g. Drake et al., 2012, 2015a,b; Iwatsuki et al., 2002; Sahlstedt et al., 2010) Groundwater flow is variable and can be slow or sporadic due to tectonic activity related to, for example,

glacioisostatic movements (e.g. Hutri, 2007) which change flow paths in fractured rock. In addition, the composition of the inflowing groundwater may change with time. This is the case in sites located around the Baltic Sea, where multiple distinct infiltrations events characterize groundwater evolution (Laaksoharju et al., 1999; Pitkänen et al., 2004). Even if these types of external forcing factors are absent, microbial activity has the ability to modify their chemical environment by reactions which otherwise would be impossible or very slow. Therefore, understanding the factors that control microbial activity in the subsurface is of primary importance in understanding geochemical evolution in deep bedrock fractures.

The Olkiluoto island on the western coast of Finland (Fig. 1) is an excellent site to study the geochemical evolution of groundwaters in bedrock fractures. Due to the ongoing site characterization and the construction of a deep geological repository intended to host spent nuclear fuel, cored boreholes have been drilled at the site for various studies. This drill core material has been sampled for the purposes of the current study. The geological history of the site during the Pleistocene and Holocene has been complex, and the bedrock fractures have been affected by several, chemically distinct infiltration events. These include, for example, glacial meltwater intrusions during the retreat of continental ice sheets, brackish water from the Baltic basin and fresh meteoric water infiltration after the area was exposed above sea level (e.g. Posiva, 2013). Consequently, the geochemical composition of infiltrating water has likely varied extensively, which has had an impact on the geochemical conditions in the deep bedrock. Information on these infiltration events has been stored in the chemical and isotopic composition of groundwaters (Posiva, 2013; Stotler et al., 2012) and fracture filling minerals (Sahlstedt et al. 2010; 2013).

Sulfur cycling in bedrock fractures is of special interest in localities where SO_4^{2-}-rich waters have been able to infiltrate into the bedrock. At Olkiluoto, SO_4^{2-} containing waters from the Baltic Sea have intruded into the bedrock (Pitkänen et al., 2004; Posiva, 2013) seen today as elevated SO_4^{2-} concentrations in groundwaters in the depth range of 150-300 m (Posiva, 2013). These SO_4^{2-}-rich

83 waters have been shown to have infiltrated during the Littorina Sea stage of the Baltic Sea (Pitkänen
84 et al., 2004) mainly during its most saline period at around 6000-3000 a (Widerlund and Andersson,
85 2011). Even earlier Pleistocene events may have introduced SO_4^{2-} into the fractures, including, for
86 example, the marine phase of the Eemian interglacial ca. 130-116 ka ago (Miettinen et al., 2002).
87 Direct evidence for bacterial sulfate reduction (BSR) in bedrock fractures at Olkiluoto has been
88 provided by observations of active microbial sulfate reducers (Haveman et al., 1999; Haveman and
89 Pedersen, 2002; Pedersen et al., 2014), and sulfur isotope signatures of dissolved sulfate (Pitkänen
90 et al., 2004; Posiva, 2013). In addition, recent sulfur isotope studies of fracture bound pyrite
91 indicated that microbial sulfate reduction has been an important process in bedrock fractures
92 repeatedly during the geological history of the site, possibly from the Paleozoic onwards (Sahlstedt
93 et al., 2013).

94 Some open questions remain about the nature of the sulfate reduction process at Olkiluoto.
95 Relatively high concentrations of SO_4^{2-} of up to 510 mg/L, remain in the deep groundwater at
96 depths of ca. 150-300 m, in a seemingly stable setting (Posiva, 2013). The reason for this stability is
97 thought to be the lack of organic compounds which could be used by microbes as electron donors in
98 SO_4^{2-} reduction (Pitkänen et al., 2004; Posiva, 2013). However, a compositional boundary between
99 SO_4^{2-} and CH_4 containing water masses at a depth of 300 m appears to be an exception. Along this
100 chemical boundary HS^- concentrations are occasionally elevated, indicating that active SO_4^{2-}-
101 reduction (Pitkänen et al., 2004) may occur by microbial mediated anaerobic methane oxidation
102 (Pedersen et al., 2008; 2014; Posiva, 2013). Furthermore, Pedersen (2013) experimentally
103 demonstrated the potential coupling of microbial anaerobic oxidation of methane to sulfate
104 reduction at a depth of 327 m in Olkiluoto. The position of this sulfate reduction zone is well
105 documented in the chemical composition of groundwaters. However, no evidence exists for the past
106 evolution of this interface.

Close to the ground surface, the bedrock fractures were saturated with SO_4^{2-}-rich waters during the Littorina Sea stage of the Baltic Sea. The SO_4^{2-} in the upper 100 m of bedrock has mostly been diluted by subsequent meteoric infiltration and partly been consumed by bacterial sulfate reduction. Fracture bound pyrite in the upper parts of the bedrock, where SO_4^{2-} concentrations are currently low, indicates that past SO_4^{2-} reduction events have occurred (Sahlstedt et al., 2013).

The carbon isotope composition of calcite in the bedrock fractures can be used to examine the substrates involved in sulfate reduction and thus more information can be gained about this important redox process in the bedrock. The aim of this study is to examine carbon cycling in bedrock fractures by analyzing the carbon isotope composition of fracture calcite *in situ* using secondary ion mass spectrometry (SIMS). The spot analyses reveal a more detailed picture of carbon isotope variability in the calcite fillings and, therefore, provide a more comprehensive picture of the processes involved compared to conventional bulk analyses (cf. Drake et al., 2015b). We especially concentrate on fracture fillings with coexisting calcite and pyrite, where earlier sulfur isotope analyses of pyrite have provided strong evidence for BSR (Sahlstedt et al., 2013).

1.1. Isotopic signature of carbon in dissimilatory sulfate reduction

BSR is a common process in anaerobic, sulfate rich environments, most notably in marine settings (e.g. Knittel and Boetius, 2009; Megonigal et al., 2005). In BSR, bacteria reduce SO_4^{2-} to S^{2-}, using organic carbon or H_2 as an electron donor. Because BSR is associated with a significant kinetic fractionation effect, analyses of the S-isotopic composition of sulfide may be applied to demonstrate the occurrence of bacterial sulfate reduction. The kinetic fractionation factor associated with BSR varies depending on the environment and micro-organisms involved (Detmers et al., 2001). Pure culture studies have shown that for some strains of bacteria the enrichment factor $\varepsilon^{34}S_{sulfate\text{-}sulfide}$ may be as high as 66‰ (Sim et al., 2011) which is in line with the large, up to ~70‰ fractionations observed in nature (e.g. Drake et al., 2015a; Wortmann et al., 2001). As a result, the bacteria tend to

strongly enrich the product sulfide in ^{32}S. If the amount of SO_4^{2-} available for bacteria is limited, the $\delta^{34}S$ values of the sulfide will become progressively higher as SO_4^{2-} is consumed in the reaction. In bedrock fractures BSR has been demonstrated by a large variation in the $\delta^{34}S$ values of low temperature pyrite (Drake et al., 2013; Sahlstedt et al., 2013). At Olkiluoto, the $\delta^{34}S$ values of pyrite in bedrock fractures varied from -50‰ to +82‰ (Sahlstedt et al., 2013) and in Laxemar, Sweden, from -50‰ to +91‰ (Drake et al., 2013). High, positive $\delta^{34}S$ values indicate a restricted SO_4^{2-} supply in the fracture network (Drake et al., 2013; Sahlstedt et al., 2013)

Sulfate reduction and carbon cycling are strongly linked because in the SO_4^{2-}-reduction process organic carbon is mineralized and transferred to the dissolved inorganic carbon (DIC) pool. In ocean water the $\delta^{13}C$ value of dissolved organic carbon (DOC) is typically low; at about -22‰ (Benner et al., 1997). In soils and aquifers, the $\delta^{13}C$ value of DOC is more variable, but typically close to -25‰ (e.g. Clark and Fritz, 1997). Degradation of organic matter will transfer this isotopic signature to the DIC.

In environments where organic carbon is mineralized in BSR, the $\delta^{13}C$ value of DIC depends not only on the bacterial contribution, but also on the other carbon sources adding to the DIC pool. The evolution of carbon isotope composition of DIC is therefore site specific and often complex. At Olkiluoto, the $\delta^{13}C$ of DIC in the present overburden varies from -27‰ to -11‰, indicating degradation of organic matter and mineral weathering, including dissolution of carbonate minerals in till and near surface fractures (Posiva, 2013). A contribution from ocean water would input DIC with a $\delta^{13}C$ value close to 0‰ (e.g. Veizer et al., 1999). Mixing between these surface-derived carbon sources could therefore lead to $\delta^{13}C_{DIC}$ values varying from about -25‰ to close to 0‰.

Anaerobic oxidation of methane (AOM) by microbes has been linked with sulfate reduction in marine sediments, where it forms an important CH_4 consuming zone at the SO_4^{2-}/CH_4 interface (e.g. Barnes and Goldberg, 1976). Even though a zone of CH_4 oxidation and SO_4^{2-} reduction is often

distinct in geochemical profiles (Barnes and Goldberg, 1976; Martens and Berner, 1974; Reeburgh, 1976), open questions remain concerning the microbial community responsible for the AOM (e.g. Antler et al., 2014). In addition to marine sediments, it is possible to find AOM also in other environments where SO_4^{2-}/CH_4 interfaces are found, such as in deep bedrock fractures (Kotelnikova, 2002). In a recent study, Drake et al. (2015) were able to connect BSR to AOM in deep bedrock fractures. Due to the low $\delta^{13}C$ values of methane ($\delta^{13}C_{CH4}$< -50‰ for bacterial CH_4, Whiticar, 1999), as well as the kinetic fractionation effect of microbial oxidation which further enriches the forming CO_2 in ^{12}C (Alperin et al., 1988; Whiticar and Faber, 1986; Whiticar, 1999), AOM will introduce significantly ^{13}C-depleted carbon into the DIC pool. Thus, anomalously low $\delta^{13}C_{DIC}$ values are usually connected to CH_4 oxidation. If carbonate minerals precipitate, they will be characterized by low $\delta^{13}C$ values, providing an archive of methane oxidation events. For example, at the Swedish site of Laxemar, fracture calcite with $\delta^{13}C$ values as low as -125‰ have been found, indicating oxidation of CH_4 deep in the bedrock (Drake et al., 2015b).

2. Study site

2.1. Geology and hydrogeochemical characteristics

The study site is located on an island just off the western coast of Finland and ca. 10 km north from the city of Rauma. The bedrock of the area is composed of metamorphosed supracrustal rocks, which belong to the Paleoproterozoic Svecofennian bedrock domain (Fig 1). The main rock types on the island are high-grade metamorphic epiclastic and pyroclastic sediments, presently occurring as gneisses and migmatitic gneisses (Fig. 1b). A detailed description of the Olkiluoto bedrock can be found in Kärki and Paulamäki, (2006). The Laitila rapakivi granite batholith and its satellite, the Eurajoki rapakivi stock are located to the east and south of the study area. The rapakivi granite intrusions are Mesoproterozoic, and the main phase of the intrusion is 1583±3 Ma old (Vaasjoki, 1996). The Satakunta Formation is located northeast of the site, a formation composed of mainly

179 sandstone deposited into an elongated fault bounded area (Kohonen and Rämö, 2005). The
180 sandstone formation continues into the Baltic Sea basin (Winterhalter, 1972) and it is estimated to
181 be ca. 1600 Ma old (Klein et al., 2014).

182 Groundwaters at Olkiluoto are approximately horizontally stratified according to their chemical
183 characteristics and composed of mixtures of waters derived from different sources (Pitkänen et al.
184 2004; Posiva, 2013). Deviations from the horizontal occur along hydraulically active zones (Fig.
185 2a). In the upper 100 m from ground surface, the groundwaters are HCO_3^--type, changing from
186 fresh (total dissolved solids, TDS<1 g/L) to brackish (1<TDS<10 g/L) with increasing depth. They
187 are relatively young (<2500a) and composed of mixtures of fresh meteoric waters, Baltic Sea water
188 and fresh evaporated water from the Korvensuo reservoir, a man made small reservoir in the middle
189 of the island, with water derived from the nearby Eurajoki river. At the depth range of 100-300 m
190 the waters are of the brackish SO_4^{2-}-type. The SO_4^{2-}-concentrations range from 123-510 mg/L
191 (Posiva, 2013). The SO_4^{2-}-rich waters infiltrated during the Littorina Sea stage of the Baltic Sea
192 (beginning at 8500 a, Björk, 2008) replacing and mixing with less saline subglacial groundwaters
193 and/or glacial melt waters (Posiva, 2013). Due to mixing with the melt waters with very low $\delta^{18}O$
194 values (estimated $\delta^{18}O$ value -22‰, Pitkänen et al., 2004) and Littorina Sea water (estimated $\delta^{18}O$
195 value -4.7‰, Pitkänen et al., 2004), the $\delta^{18}O$ values of the SO_4^{2-}-type groundwaters are locally very
196 low, down to -15.9‰ (Posiva, 2013). This meltwater dilution also affects the brackish Cl-type
197 groundwaters. At depths of 300 m and deeper, the groundwaters are of the brackish Cl-type,
198 turning to saline at depths of >400 m. The brackish Cl-type groundwaters are considered to be
199 diluted ancient brine (TDS>100 g/L), present at depths of >1 km in the bedrock of Olkiluoto
200 (Posiva, 2013). The brackish Cl and saline water types have a high Br/Cl ratio, indicating they
201 possibly originate from evaporitic residual fluids (Pitkänen et al., 2004; Posiva, 2013). The saline
202 and brackish waters (or the original brine) have been diluted by fresh water infiltrations with a
203 colder climate signature compared to the present day and have also been affected by water-mineral

204 interaction (Posiva, 2013). For further details on the composition and evolution of the Olkiluoto
205 groundwaters, the reader is referred to Posiva, (2013) and Pitkänen et al., (2004).

206

207 2.2. Sulfate reduction and microbial activity at Olkiluoto

208 Active microbial communities have been found at Olkiluoto (Bomberg et al., 2015; Haveman et al.,
209 1999; Haveman and Pedersen, 2002; Nyyssönen et al., 2012; Pedersen et al., 2014; Posiva, 2013).
210 Within the current geochemical environment, different microbial communities dominate at different
211 depths (Pedersen et al., 2014; Posiva, 2013). Sulfate reducing bacteria (SRB) are found at both
212 shallow depths and at the depth range of 200-400 m (Pedersen et al. 2014). SRB are most numerous
213 at the interface of the SO_4^{2-}-rich and CH_4-containing groundwaters (Pedersen et al., 2014). At the
214 same depth range there is also a peak in sulfide concentrations (Posiva, 2013). Microbial studies
215 conducted at Olkiluoto strongly suggest that sulfate reduction is significant at this depth and related
216 to the occurrence of both SO_4^{2-} and CH_4 in the water mass (Posiva, 2013). A possible pathway for
217 SO_4^{2-} reduction at the SO_4^{2-}/CH_4 interface is anaerobic methane oxidation, where microbes use CH_4
218 and possibly also other short chained hydrocarbons as electron donors (Posiva, 2013). At shallower
219 depths, where SO_4^{2-}-reducing bacteria are also encountered, electrons are likely provided by organic
220 carbon compounds transferred into the fractures with the infiltrating waters.

221 In addition to microbial studies, the isotopic composition of SO_4^{2-} in groundwaters indicates that
222 bacterial sulfate reduction has occurred at Olkiluoto. In the overburden and the shallower parts of
223 the bedrock, SO_4^{2-}concentration is low, typically <100 mg/L, and derived from oxidation of organic
224 material and sulfide minerals (Posiva, 2013). Most of the SO_4^{2-} in the Olkiluoto groundwaters is
225 concentrated at the depth range of 100-300 m and represent the remains from the infiltration of the
226 Littorina Sea water. At these depths, the SO_4^{2-} concentrations are on average 356 mg/L. Sulfur and
227 oxygen isotope compositions of the dissolved SO_4^{2-} indicate that BSR has occurred (Posiva, 2013).

For example, $\delta^{34}S$ values as high as +36‰ are found at depths of >150 m and the average value of the Littorina derived SO_4^{2-} is +25.8‰ (Pitkänen et al., 2004). Similarly, the $\delta^{18}O$ values of SO_4^{2-} have increased due to BSR, interpreted from the covariation of $\delta^{34}S$ and $\delta^{18}O$ values in SO_4^{2-} (Posiva, 2013).

In overburden and shallow bedrock, the $\delta^{13}C$ values of DIC range from -27.5‰ to -5.8‰ (Fig. 2). In the fresh and brackish HCO_3^--type groundwaters the $\delta^{13}C_{DIC}$ values have a narrower range, from -18.6‰ to -12.2‰ (Fig. 2, Posiva, 2013). The $\delta^{13}C_{DIC}$ values indicate input from the degradation of organic carbon, which in the upper parts of the bedrock is the most likely substrate used in BSR. However, minor amounts of CH_4 oxidation may occur which is not shown in the $\delta^{13}C_{DIC}$ values of the mixed DIC pool. The DIC content of the deep groundwaters is low, typically <20 mg/L at depths of >100m, and therefore, $\delta^{13}C_{DIC}$ data from the deep groundwaters are scarce. Even though other geochemical data and microbial studies indicate that anaerobic methane oxidation occurs, it is not reflected in the few $\delta^{13}C_{DIC}$ values obtained from these depths. One very low $\delta^{13}C$ value of -36‰ has been analyzed from the SO_4^{2-}-type waters, representing the only C isotopic indication of possible CH_4 oxidation (Posiva, 2013). Typically, at depths >100 m, the $\delta^{13}C_{DIC}$ values vary between -25‰ and -10‰ (Posiva, 2013).

2.3. Mineralogical evidence on sulfate reduction at Olkiluoto

Fracture filling calcite was divided into five groups according to mineral associations, morphology and sequence of precipitation (Sahlstedt et al., 2010). Pyrite is associated with all of the calcite groups (Sahlstedt et al., 2010; 2013). Group 1-2 calcite fillings represent the latest mineral fillings in the fracture surfaces and are composed of small euhedral crystals or thin platelets (Group 1) which may contain small amounts of silicate impurities (Group 2). Group 1-2 calcite fillings precipitated at low temperatures, indicated by the lack of two phase (liquid and vapor) primary inclusions (<80 °C, Roedder, 1984). The isotopic composition of group 1-2 calcite and pyrite have

252 more variation, compared to the massive ~1-20 mm thick calcite growth layers classified into
253 groups 3, 4 and 5 (Sahlstedt et al. 2010; 2013).

254 Mineralogical evidence of past redox conditions has been obtained from fracture mineral studies
255 (Sahlstedt et al., 2010; 2013). The $\delta^{13}C$ values of late-stage fracture filling calcite (Groups 1-2)
256 indicate that a methanogenetic environment prevailed earlier at a shallower depth compared to the
257 current situation (Sahlstedt et al., 2010). High $\delta^{13}C$ values indicate methanic conditions at depths of
258 around 50 m, when, in comparison, the CH_4 concentrations presently begin to rise at depths of ca.
259 300 m in the fracture network (Posiva, 2013). Low $\delta^{13}C$ values from fracture calcite, analyzed by
260 conventional methods, which could be related to methane oxidation have been very rare, with only
261 one Group 1 sample at the depth of 16 m having a $\delta^{13}C$ value of -30.3‰ (Sahlstedt et al., 2010).

262 Evidence from the $\delta^{34}S$ values of fracture pyrite have indicated a complex system of SO_4^{2-} reduction
263 and this is reflected in the extensive range of $\delta^{34}S$ values analyzed form late-stage pyrite, which is
264 from -50‰ to +78‰ (Sahlstedt et al., 2013). Sulfate reduction has in certain fractures proceeded
265 close to complete consumption of the SO_4^{2-}, as evidenced by highly positive $\delta^{34}S$ values of up to
266 +78‰ for Group 1 (Sahlstedt et al., 2013). In some fracture pyrite grains, reversals of the $\delta^{34}S$
267 trends have indicated repeated infiltrations of new SO_4^{2-} after the original SO_4^{2-} had been largely
268 consumed (Sahlstedt et al., 2013). These trends were thought to reflect the heterogenic flow
269 properties of the bedrock, possibly affected by glacioisostatic movements.

270 Interestingly, the $\delta^{34}S$ values of pyrite in Group 3 showed a similar distribution as those in the late-
271 stage, Group 1-2 pyrite, varying from -40‰ to +82‰ (Sahlstedt et al., 2013). Group 3 fillings
272 formed at moderate temperatures (Sahlstedt et al., 2010; 2013) and were thought to be related to
273 Paleozoic burials, during which wide areas of the Fennoscandian Shield were thought to have been
274 covered by sedimentary deposits originating from the eroding Caledonides (Larson and Tullborg,
275 1998; Larson et al., 1999; Tullborg et al., 1995). Group 3 fillings have similar characteristics as

276 fracture fillings in different localities within the Fennoscandian Shield (Sahlstedt et al., 2013), for
277 which isotope geochronometric data indicates fluid circulation especially in the Silurian and early
278 Devonia (Drake et al., 2009; Sandström et al., 2009; Alm et al., 2005). The wide variation in the
279 $\delta^{34}S$ values of the pyrite suggests that BSR was active in the fractures during the precipitation of
280 Group 3 fillings (Sahlstedt et al., 2013).

281 ## 3. Materials

282 Calcite samples were selected from the drill core material obtained from Olkiluoto. Primary
283 selection was aimed at the samples for which S-isotope data were available (Sahlstedt et al., 2013)
284 and included 23 fracture fillings in total. Additional samples were selected based on calcite type and
285 depth range (six samples) and from fractures with a black pigment, possibly representing early
286 stages of sulfide precipitation (three samples). The samples were collected from 22 different drill
287 cores obtained from bore drillings at the central and eastern parts of the island (Fig. 1b) and cover a
288 depth range from 5 m (below sea level, b.s.l.) to 527 m (b.s.l.). The samples also allow comparison
289 between the Group 1-2 and Group 3 fillings, which both had indicated the influence of BSR in a
290 previous study (Sahlstedt et al., 2013).

291 ## 4. Methods

292 ### 4.1. Sample preparation

293 A cross section of calcite fillings was needed for the in situ carbon isotope analysis. The samples
294 were prepared from 2-4 mm thick rock sections, cut perpendicular relative to the fracture surface.
295 Suitable subsamples were selected from the sections, containing typically a few mm thick areas of
296 the filling, which was cut from the rock slides and attached on epoxy buttons. Standards were
297 attached to the same sample buttons prior to SIMS analyses.

298 Prior to SIMS analyzes, the calcite samples were analyzed with an electron microscope at the
299 Geological Survey of Finland, in order to obtain back scattered electron images (BEI) of the
300 samples. Possible compositional variations of the calcite can be observed in the BEI, which can
301 then be used in the selection of the spots for the C-isotope analysis. The samples were analyzed
302 under low vacuum conditions to avoid the need for sample coating.

303 4.2. Isotope analysis

304 Carbon isotope analyses were performed in several analytical sessions using a CAMECA IMS 1280
305 large geometry SIMS at the NordSIM facility in Stockholm, Sweden. A critically focused ca. 3 nA
306 Cs^+ primary beam with 20 keV impact was used to sputter the sample, and a low-energy electron
307 flooding gun was used for charge compensation. The primary beam was homogenized using a 10
308 µm raster, resulting in a ca. 15 µm analytical spot. Each analysis consisted of an initial pre-sputter
309 over a rastered 20 µm area to remove the gold coating, followed by centering of the secondary
310 beam in the field aperture (field of view on the sample of 30 µm with 90x magnification
311 transmission ion optics). Secondary ion signals were measured in the multicollector mode using a
312 Faraday detector for $^{12}C^-$ (ca. 2 x 10^7 cps), and an ion counting electron multiplier for $^{13}C^-$ at a mass
313 resolution of ca. 4000, sufficient to resolve ^{13}C from $^{12}C^1H$. A within run correction was made for
314 EM gain drift using the pulse height analysis curve. The secondary magnet field was locked at high
315 stability using an NMR field sensor operating in regulation mode. All pre-sputter, beam centering
316 and data acquisition steps were automated in the run definition. Typical internal precision obtained
317 for individual run $^{13}C/^{12}C$ ratios from twenty-four cycles of 4-second integrations was ca. 0.2 ‰
318 (SE). The sample chamber vacuum was maintained at $<2\times10^{-8}$ mbar.

319 Fully automated sequences comprised two measurements of the reference carbonate, Brown Yule
320 Marble calcite (BYM, kindly provided by J. Craven, University of Edinburgh), bracketing six
321 measurements of unknown targets. The regularly interspersed BYM measurements were used to

correct measured isotope ratios for any drift during the analytical session (typically a cubic polynomial fit was made to the standard analyses) and for instrumental mass fractionation (IMF), assuming $\delta^{13}C_{PDB}$ = -2.28‰ (J. Craven, personal communication). External precision on $\delta^{13}C$ was <0.3‰ (SD). In total, 322 unknown target spots were measured. The results are reported against the Vienna Pee Dee Belemnite (VPDB) standard, in per mil, using the δ-notation defined as:

$$\delta^{13}C\text{sample} = [(^{13}C/^{12}C\text{sample})/(^{13}C/^{12}C\text{standard} - 1)] \times 1000 \qquad \text{Eq. (1)}$$

5. Results

The $\delta^{13}C$ values of calcite ranged from -53.8‰ to +31.6‰ (Table S1 and S2 in the Supplementary Material). The highest and the lowest $\delta^{13}C$ values occurred in the fracture fillings of the upper 110 m of bedrock and were associated with the youngest fracture calcite generations. The $\delta^{13}C$ values also varied extensively within a single calcite filling, by up to 38.6‰ (Table S1).

The $\delta^{13}C$ values of the calcite fillings were divided into groups which follow the sequence of calcite generations at Olkiluoto. The most recent calcite Groups 1 and 2 had the largest variations in the $\delta^{13}C$ values, from -53.8‰ to +31.6‰ (Fig. 3). Similar highly positive $\delta^{13}C$ values had been reported from bulk sample analysis of Olkiluoto calcite fillings in a previous study (Sahlstedt et al. 2010), but the highly negative $\delta^{13}C$ values had not been reported in earlier studies (Fig. 3, Table S1). The low (<-30‰) $\delta^{13}C$ values were restricted to two fracture fillings, one of which contained calcite with anomalously negative $\delta^{13}C$ values of <-50‰.The $\delta^{13}C$ values of calcite in Group 3 showed less variation, from -22.1‰ to +11‰ (Table S1). Also in Group 3, calcite fillings showed large variations in the $\delta^{13}C$ values within single fillings, spanning a range of 21.0‰.

Figure 4 presents the isotope composition of the calcite with respect to sample depth. The $\delta^{13}C$ values of Group 1-2 calcite had a relatively narrow range in the upper parts of the bedrock, ranging from -22.5‰ to -6.9‰ at >34 m, but varied from highly negative to values close to 0‰ between 34 and 61 m. The lowest $\delta^{13}C$ values were present only locally in some fillings (Fig. 5). Below 61 m,

positive $\delta^{13}C$ values were found in several fillings. At the depth of 102 m the highest $\delta^{13}C$ value reached +31.6‰ (Fig. 4). The $\delta^{13}C$ values of Group 3 calcite varied from -22.1‰ to +11.0‰. Compared to Group 1-2 calcite fillings, the $\delta^{13}C$ values of Group 3 calcite fillings had a smaller range and did not show similar distinct variation with depth (Fig. 4). At depths of >297 m, the $\delta^{13}C$ values of Group 1-2 and Group 3 calcite showed a similar range.

For comparison, two samples were analyzed from the earliest calcite fillings presented by Group 4 and Group 5. Within these samples, the variation the $\delta^{13}C$ values was limited, spanning from -13.7‰ to -2.4‰ in Group 5 and from -13.9‰ to -13.4‰ in Group 4 (Table S1).

6. Discussion

6.1. Isotopic evidence for carbon sources in bedrock fractures

The notably large range of 85‰ in the $\delta^{13}C$ values of the calcite fillings clearly indicates the influence of multiple C-sources in deep groundwaters. Furthermore, this variation mostly characterizes Group 1-2 calcite (Fig. 3), suggesting that it reflects processes occurring at low temperatures. Figure 4 illustrates the fact that the $\delta^{13}C$ values of Group 1-2 calcite show a systematic variation with depth, which is not seen in Group 3 calcite (Fig. 4). Both Group 1-2 and Group 3 calcite fillings are typically associated with pyrite having large variation in their $\delta^{34}S$ values (Fig. 6), which indicates isotopic effects caused by kinetic fractionation in BSR (Sahlstedt et al., 2013). The variation patterns in the $\delta^{13}C$ values of the associated calcite, however, bring up distinct differences in associated microbial processes. Figure 6 also shows the carbon isotope data from conventional analyses (Table S3 in the Supplementary Material) gathered from Olkiluoto. Comparison with the bulk and SIMS analyses shows that the SIMS data follow the general outline established by the bulk data, but the conventional analyses are able to hide important details of the isotopic variation (Fig. 6).

370

371 6.2. Sources of carbon in late-stage calcite fillings

372 6.2.1. Near surface environment

373 The $\delta^{13}C$ values of late-stage calcite (Group 1-2) at depths of <34 m vary from -30.3 ‰ to -5.5 ‰
374 (Fig. 4), with most values being between -12‰ and -20‰. The low $\delta^{13}C$ values indicate input from
375 the degradation of surface derived organic matter. Based on the recent geological history of the site,
376 the organic carbon could have been infiltrated from either terrestrial or marine sources. High
377 concentrations of SO_4^{2-} have been available only when the area was submerged under sea water,
378 because of the lack of sulfate minerals in the bedrock and in the overlaying Quaternary sediments
379 (Posiva, 2013). The marine episodes include the brackish Littorina Sea stage in the Holocene
380 (Björk, 2008) and an earlier marine connection during the Eemian interglacial (Miettinen et al.,
381 2002). It is plausible that organic matter used by BSR has been partly derived from the infiltrating
382 SO_4^{2-}-rich waters. During the fresh water stages, the input of SO_4^{2-} has been reduced, limiting the
383 progress of BSR.

384 Locally, $\delta^{13}C$ values as high as -5.5‰ were recorded in calcite from the shallow bedrock fractures.
385 Such high values indicate that, in addition to organic matter degradation, also sources less depleted
386 in ^{13}C were added to the DIC pool. During the brackish Littorina Sea stage, the $\delta^{13}C_{DIC}$ value of the
387 infiltrating brackish water has been estimated to be -1‰ (Pitkänen et al., 2004). In the Eemian,
388 Fennoscandia was an island due to a connection to the North Atlantic and to the Barents Sea
389 (Miettinen et al., 2002), and the $\delta^{13}C_{DIC}$ was ca. 1‰ (Poore et al., 2006). Marine DIC contribution
390 could thus explain the variation in the $\delta^{13}C$ values of calcite. The $\delta^{18}O$ values of the (bulk) calcite
391 (Sahlstedt et al., 2010, 2013; Table S3), do not, however, suggest precipitation from Littorina or
392 ocean water, as this would have been seen as $\delta^{18}O$ values of about -5‰ (PDB) or higher in the
393 calcite, depending on the precipitation temperature. Nevertheless, a possible contribution from a

394 marine water source cannot be ruled out based on the $\delta^{18}O$ values of the calcite, as the marine
395 oxygen isotope signature may have been masked by mixing with fresh waters during infiltration
396 (decreasing the $\delta^{18}O$ value of the source water) or by the bulk analysis of the calcite material. In situ
397 oxygen isotope data on the calcite fillings may have shed some additional light on the issue, but
398 these were, unfortunately, not measured. Another possible source for ^{13}C-enriched carbon is the
399 dissolution of old carbonate minerals in the overburden or in the upper parts of the fracture network.
400 Recycling of old carbonate material can be assumed to dominate in cases when the island was
401 exposed and uplifted above the sea level and the infiltrating waters were of meteoric origin.

402 6.2.2. Methane

403 Two shallow fracture fillings at depths of 34-54 m show unusually low $\delta^{13}C$ values. The
404 anomalously low $\delta^{13}C$ values of -53.8‰ (Fig. 5a), at a depth of 34 m, clearly indicate input from
405 oxidation of methane (cf. Whiticar, 1999). Additionally, at the depth of 54 m, a calcite filling had
406 $\delta^{13}C$ values as low as -36.5‰ (Fig. 5b), which is lower than is typically expected for oxidation of
407 organic matter (cf. Clark and Fritz, 1997) and suggests a mixed source with a contribution from
408 CH_4 oxidation. Calcite fillings with a CH_4 signature showed >25 ‰ variation in $\delta^{13}C$, and unusually
409 low values were observed only locally (Fig. 5), indicating that the source of carbon has fluctuated
410 during the precipitation of the calcite fillings. The highest $\delta^{13}C$ values of calcite in these fractures
411 were from -15.3‰ to -10.9‰ (Fig. 4), which is similar to the $\delta^{13}C$ values of calcite in the upper
412 parts of the fractured bedrock. The large range in the $\delta^{13}C$ values at these depths could be attributed
413 to variable contributions of methane derived carbon. As a whole, the contribution from CH_4
414 oxidation seems to have been minor and restricted to a few fractures.

415 Anaerobic methanotrophy is the dominant sink for CH_4 in modern marine sediments. The process is
416 operated by a consortium of methane-oxidizing archaea and sulfate-reducing bacteria (Hinrichs and
417 Boetius, 2002) and can also operate in other environments where a sulfate-methane interface is

found (Drake et al., 2015b; Kotelnikova, 2002). The sulfur isotope data from fracture pyrite indicate that there was BSR at shallow depths of <34 m in the bedrock fractures (Sahlstedt et al., 2013), and thus also anoxic conditions. Calcite fillings with methane oxidation derived carbon also contained pyrite as seen in Fig 5a, with sulfur isotopic evidence for BSR (Sahlstedt et al., 2013), suggesting a connection between BSR and methane oxidation.

Highly positive $\delta^{13}C$ values of fracture calcite were found at depths of >100 m (Fig. 4), but $\delta^{13}C$ values close to 0‰ are found already at depths of 61 m (Table S1, Sahlstedt et al., 2010). The positive $\delta^{13}C$ values indicate that the calcite precipitated from a DIC pool which was enriched in ^{13}C. Enrichment of ^{13}C in low temperature environments is commonly caused by microbial methanogenesis (e.g. Irwin et al., 1977). Due to large kinetic fractionation associated with microbial methanogenesis (e.g. Whiticar, 1999), the residual (CO_2 reduction pathway) or product CO_2 (fermentation pathway) is enriched in ^{13}C (Whiticar et al., 1986). As a result, calcite precipitating in this environment would have high $\delta^{13}C$ values (Sahlstedt et al. 2010).

6.3. Calcite fillings of Group 3

Group 3 calcite fillings, having $\delta^{13}C$ values ranging from -22.1‰ to +11.0‰, predate Group 1-2 calcite, which is indicated by the sequence of mineral formation in fractures. Figure 3 shows the distribution of the $\delta^{13}C$ values of Group 3 fillings, and the prevalence of low values of the fillings indicate that the main carbon source was degradation of organic matter. The depth distribution of the $\delta^{13}C$ values of Group 3 calcite suggests that waters containing organic compounds circulated to depths of at least 550 m. In contrast to Group 1-2 fillings, Group 3 fillings do not show anomalously low $\delta^{13}C$ values resulting from methanotrophic carbon input. The $\delta^{34}S$ values of pyrite of the same fillings indicated BSR, similar to Group 1-2 fillings (Sahlstedt et al., 2013). Therefore,

441 the C isotope composition of Group 3 calcite fillings suggests that bacteria used surface derived
442 organic matter as substrates in SO_4^{2-} reduction.

443

444 6.4. Changes in carbon cycling in bedrock fractures indicated by fracture filling minerals

445 Group 3 fillings, and the late-stage Group 1-2 fillings, have both been associated with environments
446 influenced by biogenic activity. Fluid inclusion data, although limited in number, indicate that
447 Group 3 fillings crystallized at moderate temperatures (T_h = 50-90 °C, Sahlstedt et al., 2010), high
448 salinity fluids (Sahlstedt et al., 2010; 2013). A high salinity, moderate temperature (T_h = 70-100 °C)
449 fluid type was earlier reported by Blyth et al. (2000). It was suggested (Sahlstedt et al. 2013) that
450 the Group 3 fillings were related to the Paleozoic event of Caledonian foreland basin stage (Larson
451 and Tullborg, 1998; Larson et al., 1999), which caused active fracture filling formation in large
452 areas within the Fennoscandian Shield, as shown by the direct dating of minerals in similar
453 assemblages as Group 3 at Olkiluoto (Drake et al., 2009; Sandström et al., 2009; Alm et al., 2005).
454 Relatively little is known about the Paleozoic sedimentary coverage in Finland, because knowledge
455 of these deposits is mostly based on indirect evidence (Kohonen and Rämö, 2005). Large parts of
456 Finland are thought to have been covered by sediments of the Cambrian to Silurian in age (Kohonen
457 and Rämö, 2005), and later by a thicker succession of clastic material from the eroding Caledonides
458 (Larson et al., 1999). In Sweden, the Paleozoic sedimentary cover is thought to have acted as a
459 source of organic matter and sulfur for the water circulating in the bedrock fractures (Drake and
460 Tullborg, 2009; Sandström and Tullborg, 2009). The $\delta^{13}C$ values of Group 3 calcite fillings indicate
461 a relatively uniform DIC pool, with a significant contribution of carbon from the degradation of
462 organic matter (Fig. 3) associated with BSR (Fig. 6). Overlaying deposits containing organic matter
463 and sulfate were a likely source of substrates for BSR.

464 Group 3 fillings were followed by the precipitation of Group 1-2 fillings on open fracture surfaces.
465 No isotope geochronometric data so far exist from the fillings, and therefore it is difficult to
466 ascertain the true age difference between presumably Paleozoic Group 3 fillings and the succeeding
467 late-stage fillings of Groups 1-2, which often form platelets of euhedral crystals on top of
468 continuous Group 3 fillings (Sahlstedt et al. 2010). A low temperature environment has prevailed in
469 the fracture bedrock of Olkiluoto probably for about tens of millions of years (Kohonen and Rämö,
470 2005) and Group 1-2 may partly represent the final stages of Paleozoic circulation and the
471 following long period of low temperature fluid circulation. The drastic change in the isotopic
472 composition of the fillings going from Group 3 to Group 1-2, gives an indication of a change in the
473 paleofluid compositions (this study, Sahlstedt et al., 2010) and evolution to a somewhat more
474 complex system with regards to carbon circulation. Variations in the $\delta^{13}C$ values of calcite
475 combined with the variations in the $\delta^{34}S$ values of associated pyrite (Fig. 6, Sahlstedt et al., 2013)
476 demonstrate that the upper parts of the bedrock have been geochemically active. The largest
477 variation in the $\delta^{34}S$ values of late-stage (Group 1-2) pyrite occur in the upper 25 m of the fractured
478 bedrock (Fig. 6). The carbon isotope data of associated calcite indicate input from degradation of
479 organic matter, thus showing that input of organic carbon from the ground surface could sustain
480 active SO_4^{2-} reduction in the shallow bedrock and that this input was sufficient to produce near
481 complete reduction of the SO_4^{2-} in the fractures. Evidence for clear methanotrophic activity,
482 possibly associated with BSR, is found at the depth of 34 m, and a potential methanotrophic signal
483 at the depth of 54 m. This data shows that CH_4 oxidation has affected restricted parts of the
484 fractures in the upper parts of bedrock and could only have made a very minor contribution to BSR.

485 There is a notable change from negative $\delta^{13}C$ values to positive ones at the depth range of 50-60 m,
486 which indicates a transition to a methanogenetic environment at this depth range (Fig. 6). Positive
487 $\delta^{13}C$ values are common in the latest fracture calcite precipitates at depths >60 m (Fig. 4, 6). In one
488 fracture at the depth of 111 m, the fracture surface of calcite with methanogenetic signature ($\delta^{13}C$

up to +12.1‰, Table S1) was covered by tiny pyrite crystals indicating that methanogenetic conditions were followed by sulfidic conditions with active BSR. Comparing mineralogical observations to the current groundwater environment provides further insight for this change observed in the mineralogical data.

6.5. Evolution of the groundwater system

The current groundwater environment is characterized by redox boundaries with active microbial communities; the first one occurs in the overburden and shallow bedrock where dissolved oxygen is consumed and the second one is at depths of ~300 m in the deep bedrock where SO_4^{2-} and deeper CH_4-containing groundwaters meet (Pedersen et al., 2014; Pitkänen et al., 2004; Posiva, 2013,). The $\delta^{13}C$ values are variable in the overburden and in the shallow bedrock indicating that multiple processes are involved in transferring carbon into the DIC pool (Fig. 2, Posiva 2013). The $\delta^{13}C$ values of the DIC in deep groundwaters, however, show no clear depth dependent trends and the change from a sulfidic to a methanic environment is not apparent in this data (Fig. 4). Instead, the occurrence of increased HS^- concentrations and activity of sulfate reducing bacteria are indicators of the redox transition at the SO_4^{2-}/CH_4 interface at depths of ~300 m, which also affects the DIC pool (Pedersen et al., 2012; Posiva, 2013).

The $\delta^{13}C$ values of late-stage calcite fillings suggests the occurrence of a stratified geochemical environment (Fig. 4), similar to that in the present-day groundwaters. However, the mineralogical data suggests a transition to a methanogenetic environment at depths of ~60 m with the occurrence of a possible methanotrophic zone at ~34 m. This zone is found at ~300 m (Fig. 2) in current groundwaters. Evidence for the transition of the methanogenetic environment into sulfate reducing at the depth range of 60-300 m is contained only in one sample (Fig. 5c). Strong zonation of the pyrite in this sample indicates complex sulfur evolution in the fracture (Sahlstedt et al., 2013).

513 Therefore, the transition from methanogenetic to sulfidic conditions may have fluctuated, with the
514 last change of this transition initiated by the infiltration of Littorina derived SO_4^{2-}-rich
515 groundwaters. Consumption of the CH_4 in the fracture network at depths of 60-300 m was not
516 recorded, possibly because the geochemical conditions did not favor calcite precipitation. Drake et
517 al. (2015b) showed that the progression of a CH_4-SO_4^{2-} interface in the bedrock, where sulfate
518 reducing bacteria primarily use methane in BSR due to the lack of other suitable substrates, can
519 effectively consume CH_4 from the fracture groundwaters and trigger the precipitation of calcite with
520 a methanotrophic signature. It is likely that a similar progression of a sulfate-methane interface did
521 not occur at Olkiluoto, instead, CH_4 from the 60-300 m depth range may have been flushed from
522 the fracture prior to the infiltration of SO_4^{2-}-rich waters.

523

524 7. Conclusions

525 The $\delta^{13}C$ values of calcite fillings were measured in situ by SIMS. The $\delta^{13}C$ values are variable,
526 ranging from -53.8‰ to +31.6‰, indicating contributions from multiple carbon sources and
527 different geochemical processes acting in the fracture network. The in situ carbon isotope analyses
528 revealed variations in the $\delta^{13}C$ values, especially in the late-stage fillings, which were masked in
529 conventional bulk analyses. The study was able to construct a more detailed picture of the carbon
530 cycling related to Group 1-2 late-stage fillings and the preceding Group 3 fillings, which both
531 precipitated in a system with BSR. Group 3 calcite fillings had $\delta^{13}C$ values ranging from -22.1‰ to
532 +11‰, with most of the values between -16‰ and -10‰. The $\delta^{13}C$ values indicate degradation of
533 surface derived organic matter. In contrast, the $\delta^{13}C$ values of late-stage calcite of Groups 1-2 varied
534 widely from -53.8‰ to +31.6‰ and showed depth dependent variation. The variation in the $\delta^{13}C$
535 values of the late-stage calcite indicate the following geochemical stratification:

1) In the shallow depth zone at < 30m, the calcite had a narrow range in the $\delta^{13}C$ values indicating consumption of surface derived organic matter in association with BSR.

2) In the intermediate depth of 34-54 m, the calcite had $\delta^{13}C$ values down to -53.8 ‰ indicating that anaerobic methanotrophic CH_4 consumption had occurred locally.

3) In the deep zone of ~60-400 m, the calcite had $\delta^{13}C$ values up to +31.6‰ indicating methanogenetic activity.

The geochemical stratification indicated by late-stage minerals differs from that in the present-day groundwaters by the depth distribution of the sulfate-methane interface. Limited evidence from mineral proxies indicate that methanogenetic conditions were succeeded by BSR in the deep zone. Based on the scarcity of calcite with a methanotrophic signature, the fracture system was likely first flushed from methane down to depths of approximately 300 m, followed by the infiltration of sulfate rich waters.

Acknowledgements

This study was funded by Posiva Oy. We wish to thank Kerstin Lindén at the Nordsim laboratory for sample preparation, Heejin Jeon for assisting with the analysis, and Sari Lukkari at the Geological Survey of Finland for assistance with SEM imaging. We wish to thank Paula Niinikoski for commenting on an earlier version of the manuscript. We wish to thank associate editor Danielle Fortin and an anonymous reviewer, whose critical comments and suggestions helped to improve the manuscript. The Nordsim ion microprobe facility in Stockholm is financed and operated under an agreement between the research councils of Denmark, Norway and Sweden and the Geological Survey of Finland, with additional support from the Knut and Alice Wallenberg Foundation. This is Nordsim publication number 441.

8. References

Alm, E., Sundblad, K. and Huhma, H. 2005. Sm-Nd isotope determinations of low-temperature fluorite-calcite-galena mineralization in the margins of the Fennoscandian Shield. SKB Rapport R-05-66. Svensk Kärnbränslehantering AB, Stockholm, Sweden, 58 p.

Alperin, M.J., Reeburgh, W.S. and Whiticar, M.J. 1988. Carbon and hydrogen isotopic fractionation resulting from anaerobic methane oxidation. Global Biogeochemical Cycles, vol. 2, p. 279-288.

Antler, G., Turchyn, A.V., Herut, B., Davies, A., Rennie, V.C.F. and Sivan O. 2014. Sulfur and oxygen isotope tracing of sulfate driven anaerobic methane oxidation in estuarine sediments. Estruarine, Coastal and Self Science, vol. 142, p. 4-11.

Barnes, R.O. and Goldberg, E.D. 1976. Methane production and consumption in anoxic marine sediments, Geology, vol. 4, p. 297-300.

Benner, R., Biddanda, B., Black, B. and McCarthy, M. 1997. Abundance, size distribution, and stable cabon and nitrogen isotopic compositions of marine organic matter isolated by tangential-flow ultrafiltration. Marine Chemistry, vol. 57, p. 243-263.

Björk, S. 2008. The late Quaternary development of the Baltic Sea basin. In: The BACC Author Team (Eds.). Assesment of climate change for the Baltic Sea Basin. Springer-Verlag Berlin Heidelberg, p. 398-407.

Blyth, A., Frape, S., Blomqvist, R. and Nissinen, P. 2000. Assessing the past thermal and chemical history of fluids in crystalline rock by combining fluid inclusion and isotopic investigations of fracture calcite. Applied Geochemistry 15, p. 1417-1337.

Blyth, A.R., Frape, S.K. and Tullborg, E.-L. 2009. A review and comparison of fracture mineral investigations and their application to radioactive waste disposal. Applied Geochemistry 24, p. 821-835.

Bomberg, M., Nyyssönen, M., Pitkänen, P., Lehtinen, A. and Itävaara, M. 2015. Active microbial communities inhabit sulphate methane interphase in deep bedrock fracture fluids in Olkiluoto, Finland. BioMed Research International, Acticle ID 979530.

Clark, I. and Fritz, P. 1997. Environmental isotopes in hydrogeology. CRC Press, Boca Raton, London, New York. 328 p.

Detmers, J., Brüchert, V., Habicht, K.S. and Kuever, J. 2001. Diversity of sulfur isotope fractionations by sulfate-reducing prokaryotes. Applied and Environmental Microbiology, p. 888-894.

591 Drake, H. and Tullborg, E.-L. 2009. Paleohydrogeological events recorded by stable isotopes, fluid
592 inclusions and trace elements in fracture minerals in crystalline rock, Simpewarp area, SE Sweden.
593 Applied Geochemistry, vol. 24, p. 715-732.

594 Drake, H., Tullborg, E.-L. and Page, L. 2009. Distinguished multiple events of fracture
595 mineralisation related to far-field orogenic effects in Paleoproterozoic crystalline rocks, Simpevarp
596 area, SE Sweden. Lithos 110, 37-49.

597 Drake, H., Tullborg, E.-L., Hogmail, K.J. and Åström, M.E. 2012. Trace metal distribution and
598 isotope variations in low-temperature calcite and groundwater in granitoid fractures down to 1 km
599 depth. Geochimica et Cosmochimica Acta, vol. 84, p. 217-238.

600 Drake, H., Åström, M.E., Tullborg, E.-L., Whitehouse, M. and Fallick, A.E. 2013. Variablity of
601 sulphur isotope ratios in pyrite and dissolved sulphate in granitoid fractures down to 1 km depth –
602 Evidence for widespread activity of sulphur reducing bacteria. Geochimica et Cosmochimica Acta,
603 vol. 102, p. 143-161.

604 Drake H., Tullborg, E.-L., Whitehouse, M., Sandberg, B., Blomfeldt, T. and Åström, M.E. 2015a.
605 Extreme fractionation and microscale variation of sulphur isotopes during bacterial sulphate
606 reduction in deep groundwater systems. Geochimica et Cosmochimica Acta 161, p. 1-18.

607 Drake, H., Åström, M., Heim, C., Bromen, C., Åström, J., Whitehouse, M., Ivarsson, M.,
608 Siljeström, S. and Sjövall, P. 2015b. Extreme ^{13}C depletion of carbonates formed during oxidation
609 of biogenic methane in fractured granite. Nature Communications 6:7020 doi:ncomms8020

610 Hallbeck, L. and Pedersen, K. 2008. Characterization of microbial processes in deep aquifers of the
611 Fennoscandian Shield. Applied Geochemistry 23, p. 1796-1819.

612 Haveman, S.A., Pedersen, K. and Ruotsalainen, P. 1999. Distribution and Metabolic Diversity of
613 Microorganisms in Deep Igneous Rock Aquifers of Finland. Geomicrobiology Journal, vol. 16 p.
614 277-294.

615 Haveman, S.A. and Pedersen, K. 2002. Distribution of culturable mircoorganisms in Fennoscandian
616 Shield groundwater. FEMS Microbiology Ecology, vol. 39, p. 129-137.

617 Hinrichs K.-U. and Boetius, A. 2002. The anaerobic oxidation of methane: New insights in
618 microbial ecology and biogeochemistry. In: Wefer, G., Billet, D., Hebbeln, D., Jørgensen, B.B.,
619 Schlüter, M. and Van Weering T. (eds). Ocean Margin Systems. Springer-Verlag, Berlin, pp. 457-
620 477.

621 Hutri, K. 2007. An approach to palaeoseismicity in the Olkiluoto (sea) area during the early
622 Holocene. PhD. Thesis, STUKK-A222. Helsinki, 64 pp. + Appencides

623 Irwin, H., Curtis, C. and Coleman, M. 1977. Isotopic evidence for source of diagenetic carbonates
624 formed during burial of organic-rich sediments. Nature, vol. 269, p. 209-213.

625 Iwatsugi, T., Satake, H., Metcalfe, R., Yoshida, H. and Hama, K. 2002. Isotopic and morphological
626 features of fracture calcite from granitic rocks of the Tono area, Japan: a promising
627 palaeohydrogeological tool. Applied Geochemistry 17, p. 1241-1257.

628 Knittel, K. and Boetius, A. 2009. Anaerobic oxidation of methane: progress with an unknown
629 process. Annual Reviews in Microbiology 63, p. 311-334.

630 Klein R., Pesonen, L.J., Salminen, J. and Mertanen, S. 2014. Paleomagnetism of Mesoproterozoic
631 Satakunta sandstone, Western Finland. Precambrian Research, vol. 244, p.156-169.

632 Kohonen, J. and Rämö, O.T. 2005. Sedimentary rocks, diabases, and late cratonic evolution. In:
633 Rämö, O.T. and Haapala, I. (Eds). Precambrian geology of Finland. Elsevier, Amsterdam, p. 563-
634 604.

635 Korsman, K., Koistinen, J., Kohonen, M., Wenneström, M., Ekdahl, E., Honkamo, M., Idman, H.,
636 Pekkala, Y. (Eds.), 1997. Suomen kallioperäkartta – Berggrundskarta över Finland – Bedrock map
637 of Finland 1:1 000 000. Geological Survey of Finland, Espoo, Finland.

638 Kotelnikova, S. 2002. Microbial production and oxidation of methane in deep subsurface. Earth-
639 Science Reviews, vol. 58, p. 367-395.

640 Kärki, A. and Paulamäki, S. 2006. Petrology of Olkiluoto. Posiva Report 2006-02, Posiva Oy,
641 Olkiluoto, 77 p.

642 Laaksoharju, M., Tullborg, E.-L., Wikberg, P., Wallin, B., Smellie, J. 1999. Hydrogeochemical
643 conditions and evolution at the Äspö HRL, Sweden. Applied Geochemistry 14, p. 835-859.

644 Larson, S.Å. and Tullborg, E.-L. 1998. Why Baltic shield zircons yield late Paleozoic , lower-
645 intercept ages on U-Pb concordia. Geology, vol. 26 (10), p. 919-922.

646 Larson, S.Å., Tullborg, E.-L., Cederbom, C. and Stiberg, J.-P. 1999. Sveconorwegian and
647 Caledonian foreland basins in the Baltic Shiel revealed by fission-track thermochronology. Terra
648 Nova, vol. 11 (5), p. 210-215.

649 Martens, C.S. and Berner, R.A. 1974. Methane production in the interstitial waters of sulfate-
650 depleted marine sediments. Science, vol. 185, p. 1167-1169.

651 Megonigal, J.P., Hiens, M.E. and Visscher, P.T. 2005. Anaerobic metabolism: Linkages to trace
652 gases and aerobic processes. In: Schlesinger, W.H. (Ed.), Biogeochemistry. Holland, H.D. and
653 Turekian K.K. (Eds.) Treatise on Geochemistry vol. 8, Elsevier-Pergamin, Oxford, p. 317-424.

654 Miettinen, A., Rinne, K., Haila, H., Hyvärinen, H., Eronen, M., Delusina, I., Kadastik, E., Kalm, V.
655 and Gibbard, P. 2002. The marine Eemian of the Baltic: new pollen and diatom data from Peski,
656 Russia, and Põhja-Uhtju, Estonia. Journal of Quaternary Science, vol. 17(5-6) p. 445-458.

657 Nyyssönen, M., Bomberg, M., Kapanen, A., Nousiainen, A., Pitkänen, P. and Itävaara, M. 2012.
658 Methanogenic and sulphate-reducing microbial communities in deep groundwater of crystalline
659 rock fractures in Olkiluoto, Finland. Geomicrobiology Journal 29, p. 863-878.

660 Pedersen, K., Ekendahl, S., Tullborg, E.-L., Furnes, H., Thorseth, I. and Tumyr, O. 1997. Evidence
661 of ancient life at 207 m depth in a granitic aquifer. Geology 25, p. 827-830.

662 Pedersen, K., Arlinger, J., Eriksson, S., Hallbeck, A., Hallbeck, L. and Johansson J. 2008. Numbers,
663 biomass and cultivable diversity of microbial populations relate to depth and borehole-spacific
664 conditions in groundwater from depths of 4-450 m in Olkiluoto, Finland. The ISME Journal 2, p.
665 760-775.

666 Pedersen, K., 2013. Metabolic activity of subterranean microbial communities in deep granitic
667 groundwater supplemented with methane and H_2. The ISME Journal, p. 1-11.

668 Pedersen, K., Bomberg, M. and Itävaara, M. 2014. Summary report, microbiology of Olkiluoto and
669 ONKALO groundwater. Posiva Report 2012-42, Posiva Oy, Olkiluoto, 102 p.

670 Pitkänen, P., Partamies, S. and Luukkonen A. 2004. Hydrogeochemical Interpretation of Baseline
671 Groundwater Conditions at the Olkiluoto Site. Posiva Report 2003-07, Posiva Oy, Olkiluoto. 159 p.

672 Posiva, 2011. Olkiluoto Site Description 2011. Posiva Oy Olkiluoto, 1028 p.

673 Posiva 2013. Olkiluoto Site Description 2011, Posiva Report 2011-02, Posiva Oy, Olkiluoto, 1101
674 p.

675 Poore, H.R., Samworth, R., White, N.J., Jones, S.M. and McCave, I.N. 2006. Neogene overflow of
676 northern component water at the Greenland-Scotland Ridge. Geochemistry Geophysics
677 Geosystems, vol. 7 (6), 24 p.

678 Reeburgh, W.S. 1976. Methane consumption in Cariaco Trench waters and sediments.
679 Environmental Science Technology, vol. 2, p. 140-141.

680 Roedder, E. 1984. Reviews in Mineralogy vol. 12, Fluid inclusions. Mineralogical Society of
681 America, Washington D.C.

682 Sahlstedt, E., Karhu, J.A. and Pitkänen, P. 2010. Indications for the past redox environments in
683 deep groundwaters from the isotopic composition of carbon and oxygen in fracture calcite,
684 Olkiluoto, SW Finland. Isotopes in Environmental and Health Studies, vol. 46 (3), p. 370-391.

685 Sahlstedt, E., Karhu, J., Pitkänen, P. and Whitehouse, M. 2013. Implications of sulfur isotope
686 fractionation in fracture-filling sulfides in crystalline bedrock, Olkiluoto, Finland. Applied
687 Geochemistry, vol. 32, p. 52-69.

688 Sandström, B. and Tullborg, E.-L., 2009. Episodic fluid migration in the Fennoscandian Shield
689 recorded by stable isotopes, rare earth elements and fluid inclusions in fracture minerals at
690 Forsmark, Sweden. Chemical Geology 266, 126-142.

691 Sandström, B., Tullborg, E.-L., Larson, S.Å. and Page, L. 2009. Brittle tectonothermal evolution in
692 the Forsmark area, central Fennoscandian Shield, recorded by paragenesis, orientation and
693 40Ar/39Ar geochronology of fracture minerals. Tectonophysics, vol 478, p. 158-174.

694 Sim, M.S., Bosak, T. and Ono, S. 2011. Large sulfur isotope fractionation does not require
695 disproportionation. Science, vol. 333, p. 74-77.

696 Stotler, R.L., Frape, S.K., Ruskeeniemi, T., Pitkänen, P. and Blowes, D.W. 2012. The interglacial-
697 glacial cycle and geochemical evolution of Canadian and Fennoscandian Shield groundwaters.
698 Geochimica et Cosmochimica Acta 76, p. 45-67.

699 Tullborg, E.-L., Larson, S.Å., Björklund, L., Samuelsson, L. and Sigh, J. 1995. Thermal evidence of
700 Caledonian foreland molasse sedimentation in Fennoscandia. Swedish Nuclear Fuel and Waste
701 Management Co (SKB), Technical Report 95-18.

702 Vaasjoki, M. 1996. The Laitila rapakivi batholith revisited: new, more precise radiometric ages. In:
703 Haapala, I., Rämö, O.T. and Kosunen, P. (eds) The seventh International Symposium on Rapakivi
704 Granites and Related Rocks, Wednesday 24- Friday 26 July, 1996, University of Helsinki, Helsinki
705 – Finland: abstrackt volume. Helsinki: University Press, p. 82.

706 Veizer, J., Ala, D., Azmy, K., Bruckschen, P., Buhl, D., Bruhn, F., Carden, G.A.F. Diener, A.,
707 Ebneth, S., Gobberis, Y., Jasper, T., Korte, C., Pawellek, F., Podlaha, O.G. and Strauss, H. 1999.
708 $^{87}Sr/^{86}Sr$, $\delta^{13}C$ and $\delta^{18}O$ evolution of Phanerozoic seawater. Chemical Geology, vol. 161, p. 59-88.

709 Widerlund, A. and Andersson, P.S. 2011. Late Holocene freshening of the Baltic Sea derived from
710 high-resolution strontium isotope analyses of mollusk shells. Geology, vol. 39 (2), p. 187-190.

711 Winterhalter, B. 1972. On the geology of the Bothnian Sea, an epeiric sea that has undergone
712 Pleistocene glaciation. Geological Survey of Finland, Bulletin 258, p. 1-66.

713 Whiticar, M.J. 1999. Carbon and hydrogen isotope systematics of bacterial formation and oxidation
714 of methane. Chemical Geology, vol. 161, p. 291-314.

715 Whiticar, M.J. and Faber, E. 1986. Methane oxidation in sediment and water column environments
716 – isotope evidence. Organic Chemistry 10, p. 756-768.

717 Whiticar, M.J., Faber, E. and Schoell, M. 1986. Biogenic Methane Formation in Marine and
718 Freshwater Environments: CO2 Reduction vs. Acetate Fermentation – Isotope Evidence,
719 Geochimica et Cosmochimica Acta vol. 50, p. 693-709.

720 Wortmann, U.G., Bernasconi, S.M and Böttcher, M.E. 2001. Hypersulfidic deep biosphere indicates
721 extreme sulfur isotope fractionation during single-step microbial sulfate reduction. Geology 29, p.
722 647-650.

723

724 Figure captions:

725 Figure 1. Geological setting. a) Geology of the Olkiluoto region. (1) Svecofennian supracrustal and
726 synorogenic plutonic rocks, (2) Svecofennian late orogenic granites, (3) sandstone, (4) rapakivi
727 granite, (5) gabbro, (6)-(8) diabase dykes (modified after Korsman et al., 1997). b) Lithological map
728 of the Olkiluoto island. The map shows the location of the drill core used in the study, with the
729 exception of cores ONK-PH2 and ONK-PH11 which were drilled along the construction tunnels for
730 the repository (ONKALO) (modified from Posiva, 2011).

731

732 Figure 2. Schematic illustration of the hydrogeochemical characteristics at Olkiluoto. a)
733 Geochemical stratification of the groundwaters. In the fracture networks infiltration proceeds deeper
734 than in less fractured bedrock. Otherwise the groundwater compositions are roughly horizontally
735 stratified (modified after Pitkänen et al., 2004). b) The $\delta^{13}C$ values of groundwaters with respect to
736 depth, divided into the respective hydrogeochemical water types. The $\delta^{13}C$ values are typically <-
737 10‰, except for few analyses from the shallow bedrock and few from the brackish Cl^--type
738 groundwaters. Also shown in the figure are the DIC and DOC (dissolved organic carbon)
739 concentrations, in mg of carbon per liter of water (mgC/L). High DOC concentrations in deep
740 groundwaters (>200 m) reflect the contribution from hydrocarbon gases and contamination from the
741 sampling hoses (after Posiva, 2013).

742

743 Figure 3. Histograms showing the distributions of $\delta^{13}C$ values in Group 3 and Group 1-2 calcite
744 fillings. The figure shows that the variation in the $\delta^{13}C$ values is larger in Group 1-2 fillings
745 compared to Group 3 fillings. The $\delta^{13}C$ values of both Group 3 and Group 1-2 fillings show a peak
746 at -18‰ to -12‰, but the peak for Group 3 fillings is more pronounced.

747

748 Figure 4. The $\delta^{13}C$ values of the calcite fillings with respect to depth. The C-isotopic compositions
749 measured by SIMS are divided between Groups 3 and 1-2. Note the depth dependent trend in the
750 $\delta^{13}C$ values of Group 1-2 calcite, which change from strongly negative to strongly positive at depths
751 of ~50-60 m. In comparison, similar trends are not apparent in the $\delta^{13}C$ values of Group 3 calcite.
752 Also, the $\delta^{13}C$ values of groundwater DIC (striped area) do not show any clear depth dependent
753 trends. The $\delta^{13}C$ values of DIC are according to Posiva (2013).

754

755 Figure 5. Back scattered electron images of calcite fillings and the variation in the $\delta^{13}C$ values. The
756 $\delta^{13}C$ values for the analysis spots are given in ‰. a) Sample OL-KR19/42.19-42.25 represents
757 Group 1 calcite. The $\delta^{13}C$ values are highly variable within the precipitate, with the lowest values
758 found at the edge of the crystals. b) Two pieces of sample OL-KR53/65.74-65.81 filling (Group 1).
759 The $\delta^{13}C$ values are highly variable within distances of <100 µm. c) Sample OL-KR38/102.46-
760 102.67 (Group 3 at the bottom and Group 1 at the surface). Positive $\delta^{13}C$ values are found at the
761 very surface of the filling. Calcite precipitation was followed by pyrite precipitation, as seen in the
762 secondary electron images showing a close up of the surface of the fillings. d) Sample OL-
763 KR24/112.64-112.69 (Group 3 at the bottom and Group 2 at the surface). The very surface of the
764 fillings contains calcite with highly positive $\delta^{13}C$ values. The dark bands seen on the top layers of
765 calcite are caused by silicate inclusions in the calcite.

766

767 Figure 6. The $\delta^{13}C$ values of calcite and $\delta^{34}S$ on pyrite with respect to sample depth. In the upper
768 diagrams are shown the $\delta^{13}C$ and $\delta^{34}S$ values of Group 3 fillings and in the lower diagrams the $\delta^{13}C$
769 and $\delta^{34}S$ values of Group 1-2 fillings. Sulfur isotope data is from Sahlstedt et al. (2013), and the
770 bulk carbon isotope data from Sahlstedt et al. (2010; 2013) and Table S3. a) The $\delta^{13}C$ values of

771 Group 3 calcite (SIMS analyzes in filled boxes, bulk values in filled circles) do not show trends
772 with respect to depth. The $\delta^{34}S$ values of Group 3 pyrite show a large variation through the sampled
773 depth range. b) The $\delta^{13}C$ values of Group 1-2 calcite show depth dependent variation, which is
774 more clearly seen in the SIMS results (dark grey) than in the bulk results (light grey). The $\delta^{13}C$
775 values vary in a narrow range at depths <30 m and change from negative to positive at depths of
776 ~50-60 m.

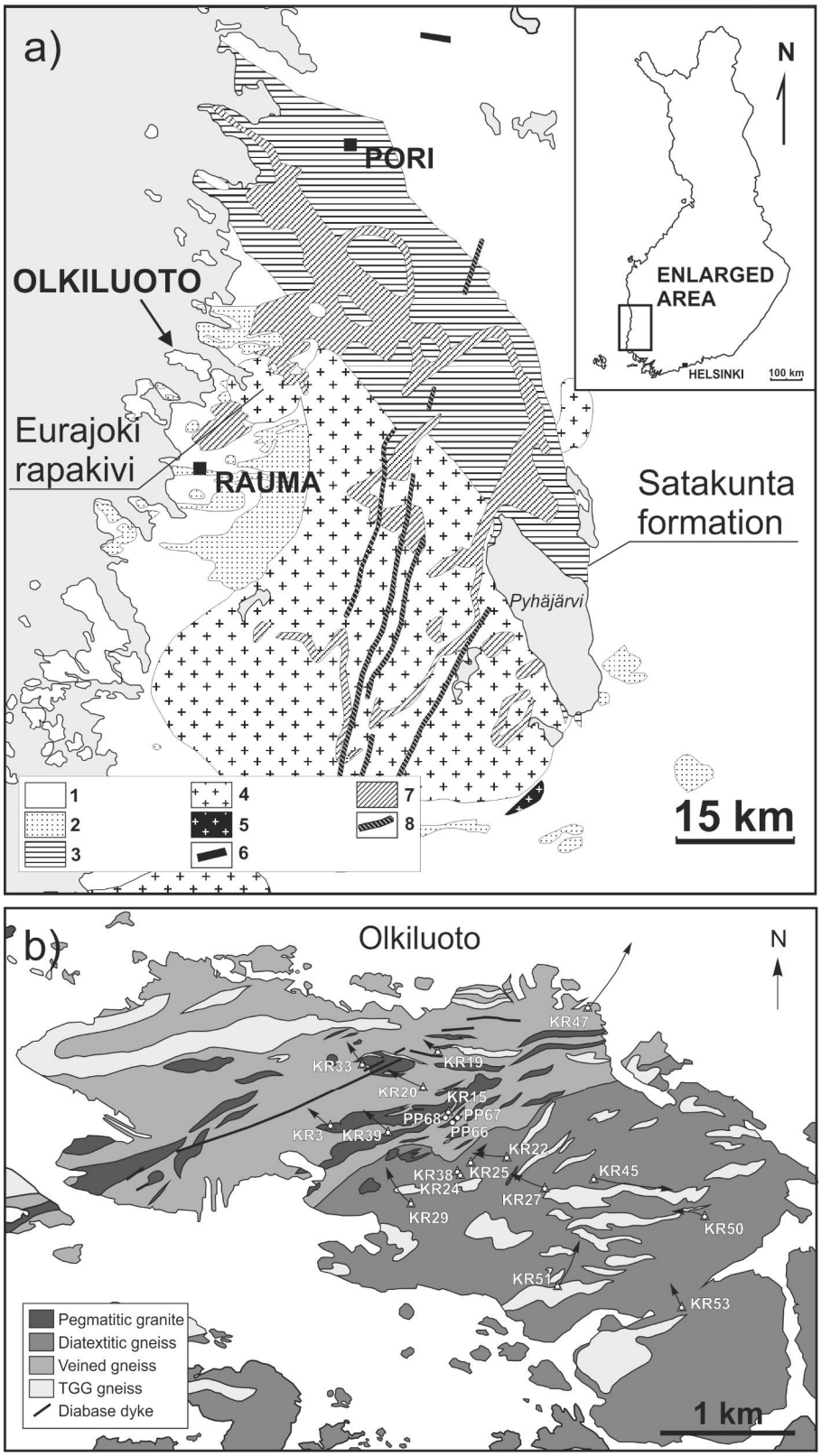

777

778 Figure 1.

779

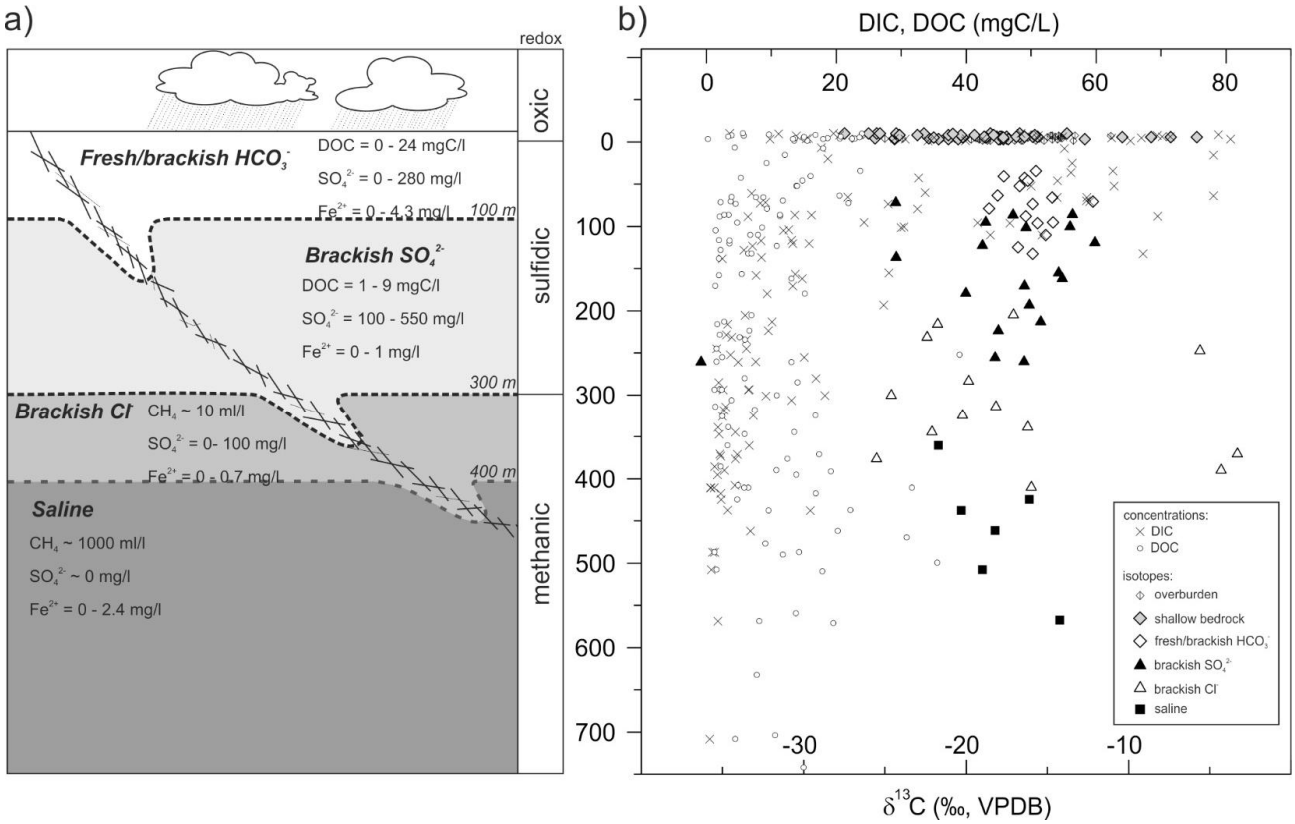

780

781 Figure 2.

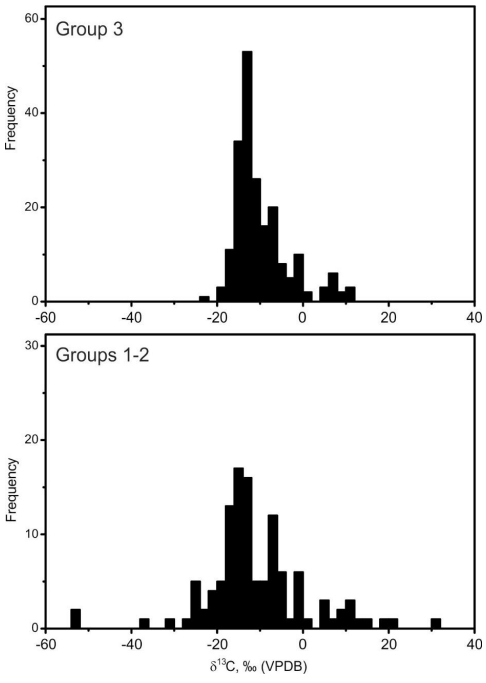

782

783 Figure 3.

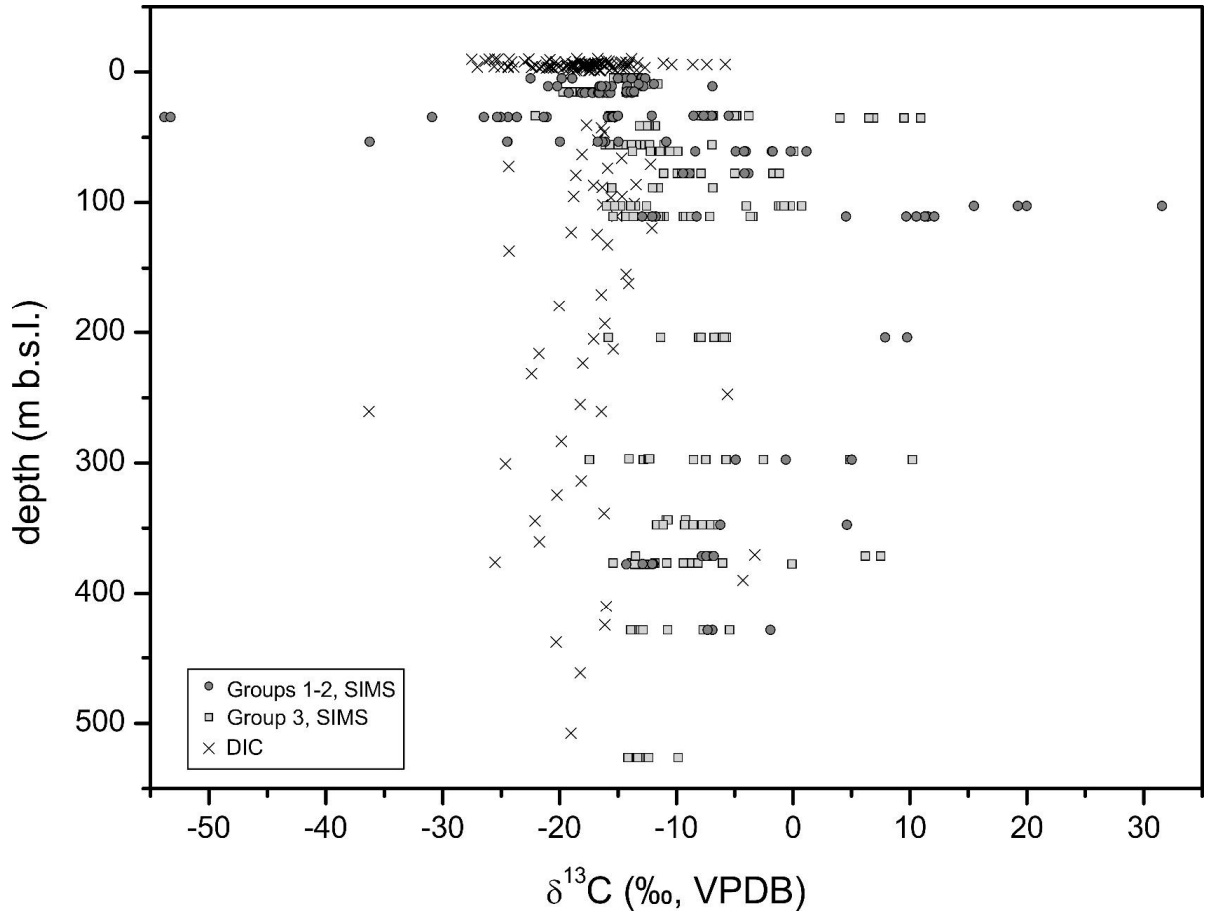

784

785 Figure 4.

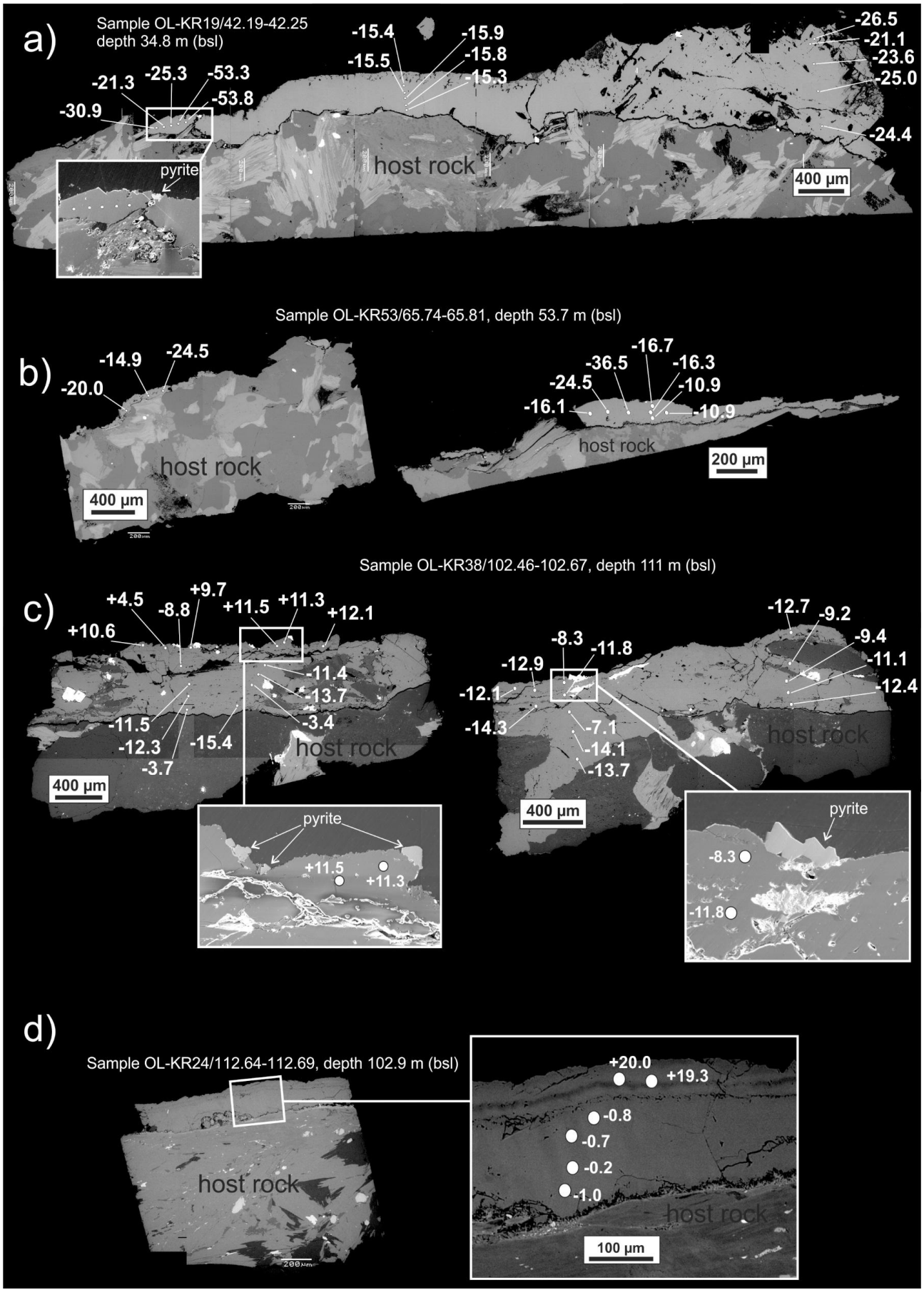
a)
Sample OL-KR19/42.19-42.25
depth 34.8 m (bsl)
-15.4
-15.9
-15.5
-15.8
-15.3
-26.5
-21.1
-23.6
-25.0
-24.4
-21.3
-25.3
-53.3
-53.8
-30.9
pyrite
host rock
400 µm
Sample OL-KR53/65.74-65.81, depth 53.7 m (bsl)
b)
-14.9
-24.5
-20.0
host rock
400 µm
-16.7
-36.5
-16.3
-24.5
-10.9
-16.1
-10.9
host rock
200 µm
Sample OL-KR38/102.46-102.67, depth 111 m (bsl)
c)
+4.5
+9.7
-8.8
+11.5
+11.3
+12.1
+10.6
-11.4
-13.7
-3.4
-11.5
-12.3
-15.4
-3.7
host rock
400 µm
pyrite
+11.5
+11.3
-12.7
-9.2
-8.3
-11.8
-9.4
-12.9
-11.1
-12.1
-12.4
-14.3
-7.1
-14.1
-13.7
host rock
400 µm
pyrite
-8.3
-11.8
d)
Sample OL-KR24/112.64-112.69, depth 102.9 m (bsl)
host rock
+20.0
+19.3
-0.8
-0.7
-0.2
-1.0
host rock
100 µm

787 Figure 5.

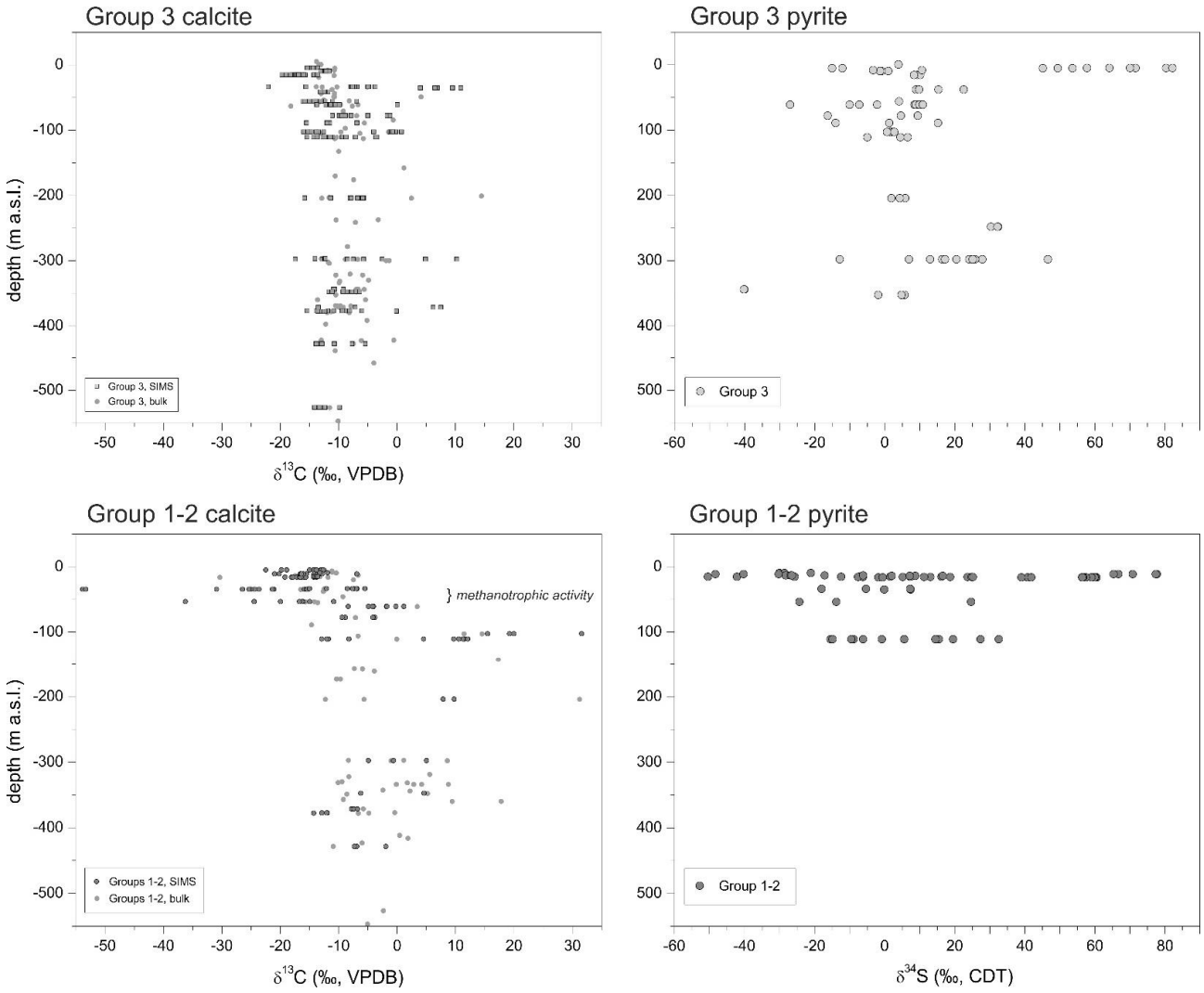

788

789 Figure 6.